Journal of Engineering and Technological Sciences

Research Paper

Hybrid Nanofluid-MQL and Cold Air Cooling for Hard Milling: RSM–PSO Multi-response Optimization

The Vinh Do[1] & Nguyen Anh Vu Le[2,*]

[1]Faculty of Mechanical Engineering, Thai Nguyen University of Technology, 666 3/2 Street, Tich Luong Ward, Thai Nguyen Province 24131, Vietnam
[2]Faculty of Mechanical Engineering, Nha Trang University, 02 Nguyen Dinh Chieu Street, Bac Nha Trang Ward, Khanh Hoa Province, 57134, Vietnam

*Corresponding author: vulna@ntu.edu.vn

Abstract

This study investigates a hybrid cooling–lubrication approach combining nanofluid-assisted minimum quantity lubrication (MQL) with cold-air cooling in the hard milling of SKD11 steel, aiming to improve both surface quality and productivity. Response surface methodology (RSM) was employed to model the relationships between machining parameters and two key performance indicators, namely surface roughness (Ra) and material removal rate (MRR). The developed models were integrated with particle swarm optimization (PSO) for multi-objective optimization. Compared with conventional MQL, the hybrid approach reduced Ra by approximately 5–10% under similar cutting conditions, indicating enhanced cooling and lubrication performance. The optimization results revealed distinct trade-offs between surface quality and productivity. When surface quality was prioritized (wRa = 0.7), a minimum Ra of 0.160 µm was achieved with a relatively low MRR of about 653 mm^3/min. In contrast, both the balanced (wRa = 0.5) and productivity-oriented (wRa = 0.3) scenarios converged to the same optimal solution (Ra ≈ 0.245 µm, MRR ≈ 1790 mm^3/min). This convergence suggests that MRR dominates the optimization when its weighting is comparable to or higher than that of Ra, indicating a plateau region on the trade-off surface. The proposed RSM–PSO framework provides both an effective optimization approach and new insight into balancing surface integrity and productivity in hybrid-cooled hard milling.

Keywords: *cold air cooling; hard milling; nanofluid MQL; PSO; RSM; SKD11.*

Introduction

Hard milling has emerged as a competitive alternative to conventional grinding in the machining of hardened tool steels. This process offers greater flexibility in machining complex geometries, reduces the number of processing steps, and has the potential to lower overall manufacturing costs (Youssef & El-Hofy, 2008; Denkena, Köhler, & Bergmann, 2015; Do & Hsu, 2016). However, it is also accompanied by considerable challenges due to elevated cutting temperatures and forces, which can accelerate tool wear, induce thermal distortions, and compromise surface integrity (Özel & Karpat, 2005; Korkut & Donertas, 2007; Davim, 2010).

In advanced manufacturing, achieving a high-quality surface finish (i.e., low surface roughness, Ra) while maintaining a high material removal rate (MRR) is a critical requirement. These two performance indicators are often conflicting, since increasing MRR generally requires higher cutting parameters that may deteriorate surface quality (Do & Phan, 2021; Vu, Hue, Huynh, & Nguyen, 2024). Therefore, developing effective cooling and lubrication strategies, along with robust optimization techniques, has become essential for balancing surface integrity and productivity in hard milling applications (Boswell, Islam, Davies, Ginting, & Ong, 2017; Dhar, Kamruzzaman, & Ahmed, 2006; Kadirgama, 2021).

Among hardened steels, SKD11 has attracted significant attention because of its high hardness, wear resistance, and dimensional stability after heat treatment (Do & Le, 2025; Nipu et al., 2023). These properties make SKD11 suitable for widespread use in dies, molds, stamping tools, and shear blades, where prolonged tool life and dimensional accuracy are crucial (Mac, Luyen, & Nguyen, 2023; Hong et al., 2021). However, the same characteristics that ensure its superior

Copyright by authors ©2026 Published by IRCS - ITB
ISSN: 2337-5779
J. Eng. Technol. Sci. Vol. 58, No. 5, 2026, 673-684
DOI: 10.5614/j.eng.technol.sci.2026.58.5.6

performance also present machining challenges, particularly in terms of tool wear and surface finish. These characteristics justify the selection of SKD11 as the workpiece material in this study.

Several cooling and lubrication strategies have been explored in hard milling to mitigate the adverse effects of high cutting temperatures and stresses. Dry cutting has often been promoted as an environmentally friendly solution, yet it typically results in excessive tool wear and poor surface finish due to uncontrolled thermal loads (Sreejith & Ngoi, 2000; Nguyen & Hsu, 2016). In contrast, flood cooling provides effective heat removal and improves surface quality but suffers from high fluid consumption and significant environmental drawbacks (Weinert, Inasaki, Sutherland, & Wakabayashi, 2004). More advanced approaches such as cryogenic cooling using liquid nitrogen (LN_2) or carbon dioxide (CO_2) can dramatically reduce cutting temperatures and enhance tool life and surface integrity. However, the required equipment and the associated costs limit their broader industrial application (Gupta, Korkmaz, Sarıkaya, Krolczyk, & Günay, 2022; Gupta et al., 2022; Ekici & Uzun, 2022).

Among sustainable alternatives, MQL has gained considerable attention. By delivering only a small quantity of lubricant directly to the cutting zone, MQL provides efficient cooling and lubrication while drastically reducing fluid usage (Boubekri & Shaikh, 2015; Abd Rahim & Dorairaju, 2018; He et al., 2023). When enhanced with dispersed nanoparticles to form nanofluid-MQL this technique has been shown to improve thermal conductivity and tribological properties, thereby reducing cutting temperatures and friction while enhancing surface quality and tool life (Godson, Raja, Lal, & Wongwises, 2010; Do & Phan, 2020; Do, 2022).

In parallel, cold-air cooling has recently emerged as another promising technique. Based on vortex-tube or compressed-air systems, it offers a clean, simple, and cost-effective alternative to cryogenic cooling, while effectively lowering cutting temperatures, stabilizing surface quality, and prolonging tool life (Chou, Liu, Chiang, & Chang, 2016; Stachurski & Nadolny, 2018; Celent, Bajić, Jozić, & Mladineo, 2023). For instance, Chou et al. (2016) demonstrated that applying a cold-air-gun cooling system during the fine grinding of Ti-6Al-4V significantly reduced thermal damage and improved dimensional accuracy. Similarly, Dong et al. (2020) reported that a minimum quantity cooling lubrication (MQCL) strategy combining emulsion-dispersed MoS_2 nanosheets with cold compressed air enhanced surface finish and tool life in the hard milling of AISI D2 steel. More recently, Celent et al. (2023) highlighted the potential of compressed cold-air cooling using a vortex tube in hard milling, emphasizing its ability to support sustainable machining while improving machinability indices. These studies underline the effectiveness of cold-air cooling as a viable alternative to conventional cooling methods in advanced manufacturing.

Taken together, these findings suggest that nanofluid-MQL and cold-air cooling are complementary approaches in advanced machining. Most existing studies have investigated nanofluid-MQL (Dong et al., 2019; Bui et al., 2024) or cold-air cooling (Chou et al., 2016; Celent et al., 2023) as separate strategies, without systematically addressing the combined effects of lubrication and heat dissipation.

Recent studies have shown that nanofluid-assisted MQL can significantly improve lubrication performance and reduce friction at the tool–workpiece interface, thereby enhancing surface quality and tool life (Salur et al., 2025; Namlu & Kaftanoğlu, 2025; Lotfi et al., 2024). However, under high thermal loads, lubrication alone is often insufficient, as elevated temperatures can still accelerate tool wear and degrade surface integrity. In this context, advanced cooling approaches such as cryogenic air and hybrid cooling systems have demonstrated strong potential for reducing cutting temperatures and improving machinability (Liu et al., 2021; Liu et al., 2023; Liu et al., 2025).

From a thermo-tribological perspective, machining performance is governed by the coupled interactions among of friction, heat generation, and material deformation. Studies have emphasized that neither lubrication-dominant nor cooling-dominant strategies alone can effectively control all of these factors simultaneously. For instance, cooling-based techniques can efficiently dissipate heat but may fail to reduce friction and adhesion, whereas lubrication-focused approaches cannot fully mitigate thermal effects under severe cutting conditions (Kumar et al., 2024; Wang et al., 2024).

Consequently, hybrid strategies that integrate multiple mechanisms have been increasingly recognized as a promising direction for sustainable machining. Recent studies have highlighted the effectiveness of combining different techniques, such as hybrid nanofluid MQL and advanced assisted-machining methods, to improve both machining performance and sustainability (Namlu et al., 2024; Lotfi et al., 2024). However, the integration of nanofluid-MQL with cold-air cooling remains insufficiently explored, particularly in the hard milling of SKD11 steel.

Furthermore, many existing optimization studies focus on single-response objectives, such as minimizing surface roughness (Do & Hsu, 2016; Nipu et al., 2023), without fully capturing the trade-off between surface quality and

DOI: 10.5614/j.eng.technol.sci.2026.58.5.6

productivity. Therefore, there is a clear need for a systematic investigation that integrates hybrid cooling–lubrication strategies with multi-objective optimization to better understand and balance these competing performance criteria.

Existing studies have also primarily focused on either lubrication or cooling independently, without fully addressing their coupled thermo-tribological interactions under high-load machining conditions. To address this limitation, this study proposes a hybrid framework that combines experimental modeling with computational optimization for hard milling. A response surface methodology (RSM) model is first established to describe the nonlinear relationships between cutting parameters (cutting speed, feed rate, depth of cut, and nanofluid concentration) and machining responses (surface roughness, Ra, and material removal rate, MRR). Particle swarm optimization (PSO) is then integrated with the RSM models to enable more flexible and effective exploration of the trade-off surface than the conventional RSM desirability function, while allowing the weighting factors assigned to Ra and MRR to be adjusted. Beyond its methodological contribution, this work experimentally validates the combined use of nanofluid-MQL and cold-air cooling in the hard milling of SKD11 steel. The overarching objective is to demonstrate how this hybrid cooling–lubrication strategy, coupled with a robust RSM–PSO optimization framework, can simultaneously improve surface integrity and productivity, thereby providing both new insights and practical guidelines for sustainable machining.

Methodology

This section describes the experimental setup, experimental design, measurement procedures, and optimization framework employed in this study.

Experimental Setup

The experiments were performed on a DMU 50 five-axis CNC milling machine using SKD11 steel with a hardness of 50 HRC (the chemical composition is presented in Table 1). A D10 TiAlN-coated end mill with four flutes, a rake angle of 12°, and a helix angle of 35° was used for the experiments. The milling operation was conducted under slotting conditions, which typically induces high thermal and mechanical loads due to full cutter engagement. The cutting length for each slot was approximately 50 mm.

Table 1 Chemical composition of SKD11 steel.

C	Si	Mn	Ni	Cr	Mo	W	V	Cu	P	S
1.4–1.6	0.4	0.6	0.5	11.0–13.0	0.8–1.2	0.2–0.5	≤0.25	≤0.25	≤0.03	≤0.03

The cooling–lubrication system combined nanofluid-based MQL with compressed cold air cooling (Figure 1). The MQL nozzle (Noga precision) was positioned at an angle of 45° and a distance of 20 mm from the cutting edge, delivering the nanofluid at a flow rate of 50 mL/h under an air pressure of 4 bar. The nanofluid was prepared by mixing canola oil with Al_2O_3 nanoparticles (20 nm, 99.9% purity) at concentrations of 0%, 1%, and 2%. The selected concentration range (0–2 wt%) was determined based on previous studies and preliminary trials to ensure stable dispersion without excessive viscosity. Al_2O_3 nanoparticles were selected because of their high thermal conductivity, chemical stability, and proven effectiveness in enhancing tribological performance in machining applications (Kumar and Krishna 2020). To ensure homogeneous dispersion, the mixture was magnetically stirred for 3 h and then ultrasonicated at 40 kHz for 30 min before use. No noticeable sedimentation was observed during the experiments, owing to the ultrasonic dispersion performed before machining. In parallel, the cold air cooling unit supplied compressed air at 6 bar and an outlet temperature of 10 °C, which was directed independently toward the cutting zone.

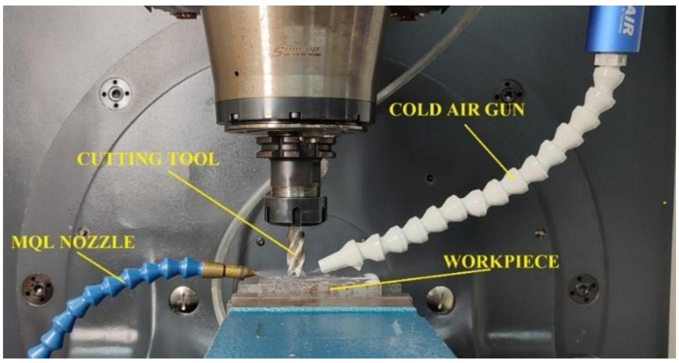

Figure 1 Schematic of the experimental setup combining nanofluid-MQL and cold air cooling.

This configuration enabled the individual application of nanofluid-MQL as well as its hybrid combination with cold-air cooling, providing the basis for evaluating their comparative and synergistic effects on hard milling performance.

Experimental Design

The experimental plan was developed based on the Box–Behnken design (BBD), which is widely adopted for response surface methodology because of its efficiency in modeling nonlinear interactions using a relatively small number of runs. Four input factors were considered: cutting speed (Vc), feed rate (f), depth of cut (a_p), and nanofluid concentration (C). In addition, the use of cold-air cooling (N: Yes/No) was incorporated as a categorical variable to evaluate its influence on machining performance. The selected parameter ranges were as follows: Vc = 40–80 m/min, f = 0.01–0.03 mm/tooth, a_p = 0.2–0.6 mm, and C = 0–2 wt%.

The responses measured in each run were surface roughness (Ra) and material removal rate (MRR), representing surface integrity and productivity, respectively. A total of 58 experimental runs were performed, including all BBD combinations and replicated center points to improve statistical reliability. The complete design matrix and the corresponding experimental results are summarized in Table 2.

Measurement Methods

After each run, Ra was measured using a Mitutoyo SJ-410 portable roughness tester (cutoff length 0.8 mm; evaluation length 4 mm). Three traces were taken along the feed direction at different locations within each slot, and the average value was reported. The variation between measurements was small, indicating good repeatability in the surface roughness measurements.

The outlet temperature of the cold-air nozzle was monitored using a GIM 3590 – LaserSight Optris infrared thermometer to ensure stable cooling during the tests. MRR was calculated from the cutting parameters using Eq. (1):

$$MRR = \frac{a_p \times a_e \times v_c \times f \times z \times 1000}{\pi \times D} \tag{1}$$

where: Vc is cutting speed (m/min), f is feed rate (mm/tooth), z is number of flutes, D is cutter diameter (mm), a_p is axial depth of cut (mm) and a_e is radial width of cut (mm).

Modeling and Optimization

This section presents the development of the regression models and the multi-objective optimization approach based on PSO.

To establish empirical relationships between machining parameters and responses, the experimental data were analyzed using response surface methodology. A second-order polynomial regression model was fitted for both Ra and MRR as functions of the input factors (Vc, f, a_p, C, and N), including linear, quadratic, and interaction terms. The adequacy of the models was evaluated through analysis of variance (ANOVA), considering the significance of model terms (p-values < 0.05), coefficients of determination (R^2, adj-R^2, pred-R^2), and lack-of-fit tests.

For multi-response optimization, the RSM regression models were coupled with particle swarm optimization (PSO). In this framework, Ra was treated as a minimization objective and MRR as a maximization objective. Both responses were normalized by their global minimum and maximum values within the studied domain, and a weighted-sum approach was applied to construct the overall objective function given in Eq. (2):

$$F = w_{Ra} \times \frac{Ra - Ra_{min}}{Ra_{max} - Ra_{min}} - w_{MRR} \times \frac{MRR - MRR_{min}}{MRR_{max} - MRR_{min}} \tag{2}$$

where w_{Ra} and w_{MRR} are the weights assigned to Ra and MRR, respectively.

The weighted-sum approach was adopted because of its simplicity and effectiveness in handling multi-objective optimization problems.

Three weighting schemes were considered: (0.5–0.5), (0.7–0.3), and (0.3–0.7), representing balanced, surface-quality–oriented, and productivity-oriented optimization scenarios, respectively. For each weighting scheme, PSO was executed

DOI: 10.5614/j.eng.technol.sci.2026.58.5.6

under both cooling conditions (N = 0 for MQL only, and N = 1 for MQL combined with cold-air cooling), and the best solution was selected based on the final objective value.

The PSO algorithm was implemented in Python using the pyswarm package with a swarm size of 30 and a maximum of 50 iterations. The optimization was performed within the specified parameter bounds: C = 0–2 wt%, Vc = 40–80 m/min, f = 0.01–0.03 mm/tooth, a_p = 0.2–0.6 mm, N = Yes/No. Unlike the traditional desirability function, which yields a single-point solution, PSO directly explores the trade-off surface and provides flexibility in identifying solutions according to the assigned weights. The integration of RSM and PSO thus combines accurate predictive modeling with robust optimization capabilites, allowing the identification of parameter settings that best satisfy different machining priorities. To ensure the robustness of the PSO algorithm, standard parameter settings were adopted, including an inertia weight (w) of 0.7 and cognitive and social acceleration coefficients of c1 = 1.5 and c2 = 1.5. These values are commonly recommended in the literature to balance global exploration and local exploitation. In addition, multiple independent runs of the PSO algorithm were performed, and consistent convergence to similar optimal solutions was observed. This result indicates that the optimization results are stable and relatively insensitive to random initialization of particles.

Results

This section presents the experimental findings and statistical modeling results, which form the basis for the subsequent discussion.

Experimental Results

The outcomes of the 58 Box–Behnken experimental runs are summarized in Table 2. The measured surface roughness (Ra) values ranged from 0.173 µm to 0.313 µm, while the material removal rate (MRR) varied between 101.91 mm³/min and 1834.39 mm³/min. These results clearly indicate that machining parameters significantly affect both surface quality and productivity. In general, higher feed rate (f) and depth of cut (a_p) increased both Ra and MRR, while cold air assistance consistently reduced Ra. Increasing nanofluid concentration (C) from 0 to 2 wt.% also contributed to improved surface finish.

Table 2 Experimental design and results.

Run Order	C %wt	Vc m/min	f mm/tooth	a_p mm	N	Ra µm	MRR (mm³/min)	Run Order	C %wt	Vc m/min	f mm/tooth	a_p mm	N	Ra µm	MRR (mm³/min)
1	1	60	0.02	0.4	No	0.246	611.46	30	2	60	0.03	0.2	No	0.236	458.60
2	0	60	0.01	0.6	Yes	0.225	458.60	31	1	60	0.02	0.4	No	0.241	611.46
3	2	80	0.02	0.4	No	0.197	815.29	32	0	60	0.03	0.4	Yes	0.296	917.20
4	1	40	0.03	0.4	Yes	0.281	611.46	33	1	80	0.02	0.2	Yes	0.199	407.64
5	2	60	0.03	0.4	Yes	0.251	917.20	34	2	80	0.02	0.2	No	0.181	407.64
6	0	40	0.02	0.6	No	0.297	611.46	35	1	40	0.01	0.2	Yes	0.187	101.91
7	1	80	0.01	0.4	No	0.183	407.64	36	0	60	0.01	0.6	No	0.247	458.60
8	2	60	0.02	0.2	Yes	0.195	305.73	37	2	60	0.01	0.2	Yes	0.173	152.87
9	1	60	0.02	0.6	No	0.25	917.20	38	1	60	0.03	0.2	No	0.263	458.60
10	0	80	0.02	0.2	Yes	0.23	407.64	39	0	80	0.02	0.4	Yes	0.244	815.29
11	1	60	0.01	0.2	Yes	0.181	152.87	40	2	40	0.02	0.2	Yes	0.207	203.82
12	2	40	0.02	0.4	No	0.223	407.64	41	1	60	0.02	0.4	Yes	0.236	611.46
13	1	40	0.01	0.6	Yes	0.226	305.73	42	0	60	0.02	0.6	No	0.282	917.20
14	0	60	0.03	0.6	No	0.313	1375.80	43	1	40	0.02	0.6	Yes	0.264	611.46
15	1	60	0.02	0.4	Yes	0.224	611.46	44	2	60	0.03	0.6	Yes	0.263	1375.80
16	2	60	0.01	0.6	No	0.184	458.60	45	1	60	0.02	0.4	Yes	0.237	611.46
17	1	80	0.02	0.6	Yes	0.23	1222.93	46	0	80	0.02	0.2	No	0.234	407.64
18	0	60	0.02	0.4	No	0.26	611.46	47	2	60	0.01	0.4	No	0.173	305.73
19	1	40	0.02	0.2	No	0.245	203.82	48	1	40	0.02	0.6	No	0.271	611.46
20	2	80	0.02	0.6	Yes	0.2	1222.93	49	0	60	0.01	0.4	Yes	0.213	305.73
21	1	60	0.03	0.6	Yes	0.298	1375.80	50	1	80	0.01	0.2	No	0.179	203.82
22	0	40	0.02	0.4	Yes	0.279	407.64	51	2	40	0.02	0.6	No	0.245	611.46
23	2	60	0.02	0.4	No	0.212	611.46	52	1	60	0.03	0.4	No	0.288	917.20
24	1	80	0.03	0.6	No	0.283	1834.39	53	0	40	0.02	0.2	Yes	0.257	203.82
25	0	80	0.02	0.6	No	0.265	1222.93	54	2	80	0.02	0.4	Yes	0.19	815.29
26	1	60	0.01	0.6	Yes	0.204	458.60	55	1	60	0.01	0.4	Yes	0.195	305.73
27	2	40	0.02	0.6	Yes	0.23	611.46	56	0	60	0.03	0.2	No	0.289	458.60
28	1	40	0.03	0.6	No	0.311	917.20	57	1	80	0.03	0.4	Yes	0.247	1222.93
29	0	60	0.02	0.2	Yes	0.239	305.73	58	2	60	0.02	0.6	No	0.227	917.20

Model Adequacy

The adequacy of the regression model for Ra was verified using analysis of variance (ANOVA). As shown in Table 3, the model was statistically significant ($p < 0.001$), with feed rate identified as the most influential factor, followed by cutting speed, depth of cut, and nanofluid concentration. Cold air assistance also had a statistically significant effect. Although several quadratic and interaction terms were not statistically significant ($p > 0.05$), they were retained to preserve the hierarchical structure of the response surface model. This approach is commonly adopted in RSM to ensure model stability and maintain predictive capability across the entire design space.

Table 3 ANOVA for Ra.

Source	DF	Adj-SS	Adj-MS	F-Value	P-Value
Model	19	0.079997	0.004210	125.98	0.000
Linear	5	0.075904	0.015181	454.23	0.000
C	1	0.019769	0.019769	591.51	0.000
Vc	1	0.006060	0.006060	181.33	0.000
f	1	0.033258	0.033258	995.13	0.000
a_p	1	0.006010	0.006010	179.82	0.000
N	1	0.000721	0.000721	21.56	0.000
Square	4	0.000072	0.000018	0.54	0.707
C*C	1	0.000016	0.000016	0.49	0.487
Vc*Vc	1	0.000045	0.000045	1.35	0.252
f*f	1	0.000000	0.000000	0.01	0.923
a_p*a_p	1	0.000010	0.000010	0.30	0.590
2-Way-Interaction	10	0.000268	0.000027	0.80	0.627
C*Vc	1	0.000001	0.000001	0.03	0.864
C*f	1	0.000000	0.000000	0.01	0.916
C*a_p	1	0.000032	0.000032	0.97	0.331
C*N	1	0.000023	0.000023	0.68	0.416
Vc*f	1	0.000000	0.000000	0.00	0.977
Vc*a_p	1	0.000020	0.000020	0.61	0.440
Vc*N	1	0.000000	0.000000	0.01	0.923
f*a_p	1	0.000123	0.000123	3.67	0.063
f*N	1	0.000008	0.000008	0.25	0.619
a_p*N	1	0.000002	0.000002	0.06	0.808
Error	38	0.001270	0.000033		
Lack-of-Fit	35	0.001153	0.000033	0.84	0.671
Pure-Error	3	0.000117	0.000039		
Total	57	0.081267			

The overall model summary statistics are presented in Table 4, indicating high coefficients of determination (R^2 = 98.44%, adj-R^2 = 97.66%, pred-R^2 = 95.97%). These values demonstrate excellent predictive performance of the quadratic regression model.

Table 4 Model summary statistics.

S	R-sq	R-sq(adj)	R-sq(pred)
0.0057811	98.44%	97.66%	95.97%

The quadratic regression equations, Eqs. (3) and (4) for Ra under the two cooling conditions (without and with cold-air cooling) are expressed as follows:

For N = No (without cold-air cooling):

$$Ra = 0.2007 - 0.0219C - 9.2\times10^{-5}Vc + 3.15f + 0.0395a_p - 0.00116C^2 - 5.0\times10^{-6}Vc^2 + 1.70f^2 + 0.0242a_p^2 + 1.3\times10^{-5}C\cdot Vc - 0.0190C\cdot f - 0.00678C\cdot a_p - 3.0\times10^{-4}Vc\cdot f - 2.7\times10^{-4}Vc\cdot a_p + 1.59f\cdot a_p \tag{3}$$

For N = Yes (with cold-air cooling):

$$Ra = 0.1865 - 0.0200C - 8.1\times10^{-5}Vc + 3.28f + 0.0424a_p - 0.00116C^2 - 5.0\times10^{-6}Vc^2 + 1.70f^2 + 0.0242a_p^2 + 1.3\times10^{-5}C\cdot Vc - 0.0190C\cdot f - 0.00678C\cdot a_p - 3.0\times10^{-4}Vc\cdot f - 2.7\times10^{-4}Vc\cdot a_p + 1.59f\cdot a_p \tag{4}$$

These regression models incorporate linear, quadratic, and interaction terms for the input variables, capturing the nonlinear effects of machining parameters on surface roughness.

DOI: 10.5614/j.eng.technol.sci.2026.58.5.6

To further validate the adequacy of the developed models, residual analysis was conducted. The residuals were examined using normal probability plots and residual-versus-predicted value distributions. The results indicated that the residuals were randomly scattered around zero and approximately followed a straight line on the normal probability plot, confirming that the assumptions of normality and independence were satisfied.

In addition, the close agreement between predicted and experimental values, together with the high R^2, adjusted R^2, and predicted R^2 values reported in Table 4, further demonstrates the reliability and predictive capability of the models within the investigated parameter range.

Graphical Results

The main effects of each parameter are illustrated in Figure 2, which indicates that feed rate was the most influential factor affecting Ra. Figure 3 presents the box plot of Ra grouped by cold-air assistance. It is evident that the median Ra decreased when cold air was applied, with narrower interquartile ranges, indicating improved surface stability under this condition.

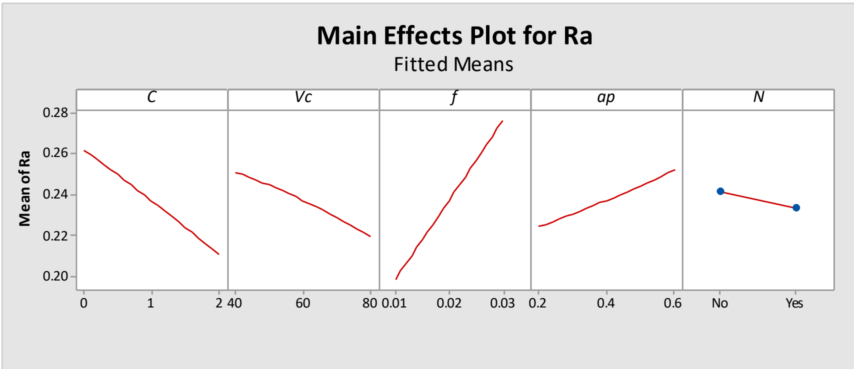

Figure 2 Main effects plot for Ra.

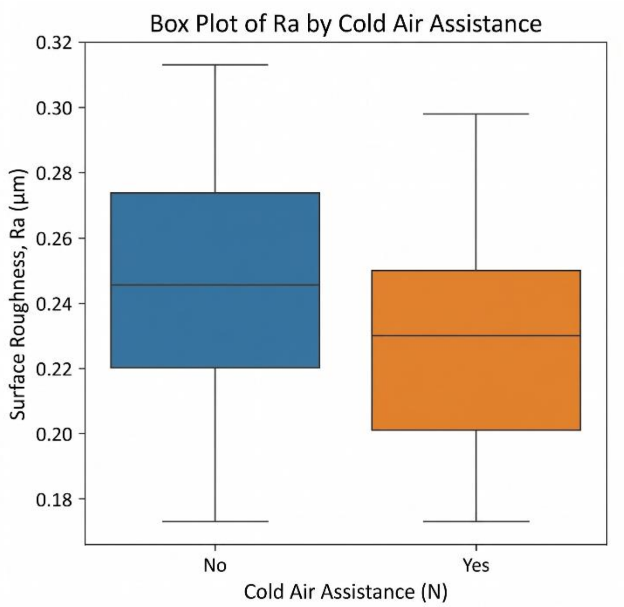

Figure 3 Box plot of Ra by cold air assistance.

Optimization Results

The PSO-based multi-objective optimization results for different weighting scenarios are summarized in Table 5. The results indicate distinct optimization outcomes depending on the relative importance assigned to surface roughness and material removal rate. When surface quality was prioritized (wRa = 0.7), the optimization yielded the lowest Ra value of approximately 0.160 µm, accompanied by a reduced MRR of about 653 mm³/min. In contrast, both the balanced (wRa = 0.5) and productivity-oriented (wRa = 0.3) scenarios converged to the same optimal parameter combination, resulting in Ra ≈ 0.245 µm and MRR ≈ 1790 mm³/min. This observation suggests that, within the investigated parameter space, increasing the weight assigned to MRR beyond a certain threshold does not further change the optimal solution, indicating a dominant influence of productivity-related parameters.

Table 5 Results of PSO-based optimization for Ra and MRR.

w_{Ra}	w_{MRR}	C (%wt)	Vc (m/min)	f (mm/tooth)	a_p (mm)	N	Ra (µm)	MRR (mm³/min)
0.5	0.5	2	80	0.03	0.6	Yes	0.2451	1790.02
0.7	0.3	2	80	0.01	0.6	Yes	0.1602	652.98
0.3	0.7	2	80	0.03	0.6	Yes	0.2451	1790.02

Discussion

This section provides a detailed interpretation of the experimental and optimization results, focusing on the influence of machining parameters and the effectiveness of the hybrid cooling–lubrication strategy. These results are particularly relevant to SKD11 steel, whose high hardness and wear resistance intensify the thermal and tribological challenges during machining. Compared with previous studies that employed MQL alone, the hybrid approach used in this study achieved lower Ra values under similar cutting conditions.

The Ra values obtained in this study ranged from 0.173 µm to 0.313 µm, indicating a relatively low surface roughness compared with dry machining conditions reported in previous works on hardened steels (Nguyen & Hsu, 2016). This improvement can be attributed to the hybrid cooling–lubrication system, which effectively reduced cutting temperatures and friction. The MRR values varied from 101.91 mm³/min to 1834.39 mm³/min, reflecting the strong influence of cutting parameters on productivity. Although cutting temperature, cutting force, and tool wear were not directly measured in this study, the observed improvement in surface roughness can be reasonably explained based on established machining mechanisms. Previous studies have shown that both nanofluid-MQL and cold-air cooling effectively reduce cutting temperatures and friction at the tool–workpiece interface, leading to more stable cutting conditions and reduced adhesion and ploughing effects.

The addition of nanoparticles enhances the thermal conductivity and lubricating performance of the base fluid, while cold air contributes to rapid heat dissipation. These combined effects are known to reduce tool wear progression and improve surface integrity. Therefore, the reduction in Ra observed in this study is consistent with the expected thermo-mechanical behavior reported in the literature.

A preliminary analysis of the experimental data revealed clear trends. Higher feed rates (f) and depths of cut (ap) generally increased both Ra and MRR, highlighting the inherent trade-off between surface quality and machining efficiency (Do & Phan, 2021; Vu, Hue, Huynh, & Nguyen, 2024). The application of cold-air cooling (N = Yes) consistently reduced Ra by approximately 5–10% compared with cases without cold air (N = No), particularly at higher cutting speeds, which may be attributed to enhanced heat dissipation. Similarly, increasing nanofluid concentration (C) from 0% to 2% improved the surface finish by reducing friction through enhanced tribological properties (Godson, Raja, Lal, & Wongwises, 2010; Do & Phan, 2020). Meanwhile, MRR—calculated using Equation (1)—was primarily governed by the product of Vc, f, and a_p, with minimal direct effects from C or N, although the hybrid cooling–lubrication system indirectly supported higher MRR by enabling more aggressive cutting parameters without excessive tool wear. It should be noted that the MRR values reported in this study were derived from theoretical calculations and do not account for potential deviations due to tool wear, vibration, or material side flow under extreme cutting conditions.

The ANOVA results (Table 3) further confirmed the statistical significance of these trends. Feed rate (f) exhibited the highest F-value (995.13, $p < 0.001$), identifying it as the most dominant factor for both Ra and MRR. According to the regression equations reported in the Results section, Ra increased almost linearly with f in the range of 0.01–0.03 mm/tooth, due to larger undeformed chip thickness and higher cutting forces. At the same time, MRR rose proportionally with f, reflecting the inevitable trade-off between productivity and surface integrity.

Cutting speed (Vc) exerted a moderate but significant effect on both responses. As shown in the regression model (Table 4), higher Vc slightly reduced Ra, as elevated temperatures may have softened the workpiece material in the shear zone, facilitating smoother chip formation. This observation is consistent with previous studies on the hard milling of tool steels (Korkut & Donertas, 2007; Nguyen & Hsu, 2016). Conversely, MRR showed a decreasing trend with increasing Vc

DOI: 10.5614/j.eng.technol.sci.2026.58.5.6

in the regression model, which can be explained by the fixed radial and axial engagement conditions in this study: Equation (1) indicates that MRR is more strongly dependent on f and a_p than on Vc.

Depth of cut (a_p) exhibited a positive correlation with both Ra and MRR. As a_p increased from 0.2 mm to 0.6 mm, Ra deteriorated moderately due to greater cutting forces and possible tool deflection, while MRR rose substantially because ap directly contributes to the volume of material removed per unit time. This confirms a_p as an important productivity-oriented parameter.

Nanofluid concentration (C) played a significant role in improving the surface finish. Increasing C from 0 wt% to 2 wt% consistently reduced Ra, as the presence of Al_2O_3 nanoparticles enhanced the both thermal conductivity and tribological properties of the MQL fluid (Godson et al., 2010; Do & Phan, 2020). This improvement was particularly evident at higher cutting speeds, where improved lubrication and heat removal were critical. However, the effect of C on MRR was negligible, since it does not directly enter the MRR equation; its main contribution was indirect, by enabling stable machining at higher f and a_p.

Cold-air assistance (N) also had a statistically significant effect ($p = 0.000$, Table 3) on Ra. Figure 3 shows that the median Ra decreased from 0.245 µm (N = No) to 0.236 µm (N = Yes), with a narrower interquartile range under cold-air cooling, indicating more stable surface quality. Although the observed difference is relatively small, it is consistent across multiple experimental runs, suggesting that the improvement is systematic rather than random measurement variation. The additional cooling effect reduced cutting temperatures and limited tool–workpiece adhesion, thereby suppressing surface roughening. While cold air did not directly affect MRR, it contributed to process stability by reducing the thermal load, which indirectly supported higher removal rates under aggressive cutting conditions.

The quadratic regression equations reported in the Results section further illustrate the nonlinear interactions among the machining parameters under the two cooling conditions. Figure 2 presents the main effects plot for Ra, clearly showing that feed rate strongly deteriorates surface finish, while higher cutting speed and nanofluid concentration reduce Ra. Depth of cut exerted a moderate negative effect. Figure 3 confirmed the beneficial role of cold air in reducing Ra, consistent with earlier reports on hybrid MQCL systems where combined lubrication and cooling yielded superior performance over standalone methods (Dong et al., 2020).

Overall, the parameter influence analysis reveals that feed rate is the primary driver of both surface roughness and productivity, whereas nanofluid concentration and cold air assistance mainly improve surface quality. Cutting speed and depth of cut play dual roles, with a_p strongly affecting productivity and Vc moderately affecting surface integrity. These findings highlight the necessity of multi-objective optimization to balance Ra and MRR in hard milling under hybrid cooling–lubrication conditions**.**

A notable finding is that the balanced and productivity-oriented scenarios converged to identical optimal solutions. This behavior is not due to computational error but reflects the intrinsic characteristics of the machining process and the optimization landscape. Specifically, MRR is strongly governed by feed rate (f) and depth of cut (a_p), both of which reach their upper bounds (f = 0.03 mm/tooth and a_p = 0.6 mm) in the optimal solution. When MRR is assigned a weight comparable to or higher than that of Ra, the optimization process consistently favors this region of maximum material removal. This indicates the presence of a plateau region on the trade-off surface, where multiple weighting scenarios lead to the same optimal solution. When surface roughness is strongly prioritized (wRa = 0.7), the optimizer shifts toward a region with lower feed rate, resulting in improved surface quality at the expense of productivity. Under this condition, the lowest Ra (≈ 0.160 µm) is achieved, but with a significantly reduced MRR (≈ 653 mm^3/min). This finding provides practical guidance for selecting machining parameters depending on whether surface quality or productivity is prioritized. An important observation is that cold air assistance was consistently included in all the optimal parameter sets, underscoring its critical role in improving surface integrity without sacrificing productivity. This finding aligns with previous research on hybrid cooling–lubrication strategies, which demonstrated superior performance compared with conventional cooling or lubrication alone (Dong et al., 2020; Celent et al., 2023).

These results confirm the effectiveness of integrating nanofluid-MQL with cold air assistance in improving both surface quality and productivity. By combining experimental analysis, regression modeling, and PSO-based optimization, the study provides both quantitative evidence and practical insights into balancing surface integrity and productivity. The implications of these results are further consolidated in the following conclusion.

It should be noted that the present study focuses on surface roughness and material removal rate as the primary performance indicators. Other important factors such as tool wear, cutting force, and cutting temperature were not experimentally measured and should be considered in future research. Incorporating these parameters would provide a more comprehensive understanding of the machining performance and further validate the underlying mechanisms of the hybrid cooling–lubrication approach.

From a sustainability perspective, the proposed hybrid approach reduces cutting-fluid consumption through the use of MQL and avoids the need for hazardous cryogenic media. Although energy consumption and the cost of compressed air were not quantitatively evaluated, the system provides a cleaner and more environmentally friendly alternative compared to conventional flood cooling.

Conclusion

This study investigated a hybrid cooling–lubrication approach combining nanofluid-based minimum quantity lubrication (MQL) with cold-air assistance for the hard milling of SKD11 steel. The results showed that feed rate and depth of cut significantly affected both surface roughness (Ra) and material removal rate (MRR), highlighting the inherent trade-off between surface quality and productivity. The hybrid system consistently improved the surface finish by 5–10% and demonstrated better overall performance compared to single-mode cooling strategies.

The integration of response surface methodology (RSM) with particle swarm optimization (PSO) enabled effective multi-objective optimization. The results revealed that different weighting scenarios could lead to similar optimal solutions, indicating the presence of a plateau region on the trade-off between Ra and MRR. This provides useful insight for selecting machining conditions based on specific production priorities. For practical applications, to achieve a surface roughness below 0.2 µm, low feed rates ($f \approx 0.01$ mm/tooth), moderate cutting speed ($V_c \approx 80$ m/min), and the use of cold air combined with a 2 wt% nanofluid are recommended. Conversely, higher productivity can be achieved by increasing feed rate and depth of cut, with an acceptable increase in surface roughness.

From an engineering perspective, the proposed hybrid cooling–lubrication approach offers a practical and environmentally friendly alternative for machining hardened steels, particularly when both surface integrity and productivity are required.

However, this study was limited to the evaluation of Ra and MRR, while tool wear, cutting force, and cutting temperature were not experimentally investigated. In addition, MRR was calculated theoretically. Future work should incorporate these factors and perform experimental validation under broader machining conditions to further enhance the industrial applicability of the proposed approach.

Acknowledgement

The authors are grateful to Thai Nguyen University of Technology for providing the necessary support and infrastructure to conduct this research.

Compliance with ethics guidelines

The authors declare they have no conflict of interest or financial conflicts to disclose.

This article contains no studies with human or animal subjects performed by the authors.

References

Abd Rahim, E., & Dorairaju, H. (2018). Evaluation of mist flow characteristic and performance in minimum quantity lubrication (MQL) machining. *Measurement, 123,* 213–225. https://doi.org/10.1016/j.measurement.2018.03.015

Boswell, B., Islam, M. N., Davies, I. J., Ginting, Y. R., & Ong, A. K. (2017). A review identifying the effectiveness of minimum quantity lubrication (MQL) during conventional machining. *International Journal of Advanced Manufacturing Technology, 92*(1–4), 321–340. https://doi.org/10.1007/s00170-017-0142-3

Boubekri, N., & Shaikh, V. (2015). Minimum quantity lubrication (MQL) in machining: Benefits and drawbacks. *Journal of Industrial and Intelligent Information, 3(3).* https://doi.org/10.12720/JIII.3.3.205-209

Bui, G.-T., Nguyen, Q. M., Thi, M. H. P., & Vu, M. H. (2024). Multi-objective optimization for balancing surface roughness and material removal rate in milling hardened SKD11 alloy steel with SiO_2 nanofluid MQL. *EUREKA: Physics and Engineering, 2,* 157–169. https://doi.org/10.21303/2461-4262.2024.003042

DOI: 10.5614/j.eng.technol.sci.2026.58.5.6

Celent, L., Bajić, D., Jozić, S., & Mladineo, M. (2023). Hard milling process based on compressed cold air-cooling using vortex tube for sustainable and smart manufacturing. *Machines, 11*(2), 264. https://doi.org/10.3390/machines11020264

Chou, C.-C., Liu, N.-M., Chiang, K.-T., & Chang, H.-C. (2016). Investigation and optimization of Ti-6Al-4V titanium alloy in the fine grinding process using cold air gun coolant system. *Hsiuping Journal, 33*, 1–28. https://libap.nhu.edu.tw:8081/Ejournal/AI01003301.pdf

Davim, J. P. (Ed.). (2010). Surface integrity in machining. *Springer.* https://doi.org/10.1007/978-1-84882-874-2

Denkena, B., Köhler, J., & Bergmann, B. (2015). Development of cutting edge geometries for hard milling operations. CIR*P Journal of Manufacturing Science and Technology, 8,* 43–52. https://doi.org/10.1016/j.cirpj.2014.10.002

Dhar, N. R., Kamruzzaman, M., & Ahmed, M. (2006). Effect of minimum quantity lubrication (MQL) on tool wear and surface roughness in turning AISI-4340 steel. *Journal of Materials Processing Technology, 172*(2), 299–304. https://doi.org/10.1016/j.jmatprotec.2005.09.022

Do, T.-V. (2022). A case study of minimizing cutting force in hard milling JIS SKD61 steel under nanofluid-MQL condition. In *Advances in engineering research and application: Proceedings of ICERA 2021*, 12–18. Springer. https://doi.org/10.1007/978-3-030-92574-1_2

Do, T.-V., & Hsu, Q.-C. (2016). Optimization of minimum quantity lubricant conditions and cutting parameters in hard milling of AISI H13 steel. *Applied Sciences, 6*(3), 83. https://doi.org/10.3390/app6030083

Do, T.-V., & Le, N. A. V. (2025). Development of a multi-objective optimization model for the hard turning of SKD11 steel with nanofluid-Al_2O_3 minimum quantity lubrication using RSM and PSO. *Engineering, Technology & Applied Science Research, 15*(4), 24897–24903. https://doi.org/10.48084/etasr.11351

Do, T.-V., & Phan, T.-D. (2020). An empirical investigation of SiO_2 nano concentration under MQL on surface roughness in hard milling of JIS SKD61 steel. *Journal of Applied Engineering Science, 18*(3), 432–437. https://doi.org/10.5937/jaes18-27335

Do, T.-V., & Phan, T.-D. (2021). Multi-objective optimization of surface roughness and MRR in milling of hardened SKD11 steel under nanofluid MQL condition. *International Journal of Mechanical Engineering and Robotics Research, 10*, 357–362. https://doi.org/10.18178/ijmerr.10.7.357-362

Dong, L., et al. (2019). Analysis of the cooling performance of Ti–6Al–4V in minimum quantity lubricant milling with different nanoparticles. *International Journal of Advanced Manufacturing Technology, 103*(5–8), 2197–2206. https://doi.org/10.1007/s00170-019-03466-y

Dong, P. Q., Duc, T. M., Tuan, N. M., Long, T. T., Thanh, D. V., & Truong, N. V. (2020). Improvement in the hard milling of AISI D2 steel under the MQCL condition using emulsion-dispersed MoS_2 nanosheets. *Lubricants, 8*(6), 62. https://doi.org/10.3390/lubricants8060062

Ekici, E., & Uzun, G. (2022). Effects on machinability of cryogenic treatment applied to carbide tools in the milling of Ti-6Al-4V with optimization via the Taguchi method and grey relational analysis. *Journal of the Brazilian Society of Mechanical Sciences and Engineering, 44*(7), 270. https://doi.org/10.1007/s40430-022-03572-1

Godson, L., Raja, B., Lal, D. M., & Wongwises, S. E. A. (2010). Enhancement of heat transfer using nanofluids—An overview. *Renewable and Sustainable Energy Reviews, 14*(2), 629–641. https://doi.org/10.1016/j.rser.2009.10.004

Gupta, M. K., Korkmaz, M. E., Sarıkaya, M., Krolczyk, G. M., & Günay, M. (2022). In-process detection of cutting forces and cutting temperature signals in cryogenic assisted turning of titanium alloys: An analytical approach and experimental study. *Mechanical Systems and Signal Processing, 169,* 108772. https://doi.org/10.1016/j.ymssp.2021.108772

Gupta, M. K., Korkmaz, M. E., Sarıkaya, M., Krolczyk, G. M., Günay, M., & Wojciechowski, S. (2022). Cutting forces and temperature measurements in cryogenic assisted turning of AA2024-T351 alloy: An experimentally validated simulation approach. *Measurement, 188,* 110594. https://doi.org/10.1016/j.measurement.2021.110594

He, T., Liu, N., Xia, H., Wu, L., Zhang, Y., Li, D., & Chen, Y. (2023). Progress and trend of minimum quantity lubrication (MQL): A comprehensive review. *Journal of Cleaner Production, 386,* 135809. https://doi.org/10.1016/j.jclepro.2022.135809

Hong, T. T., Vinh, D. T., Hung, T. V., Giang, T. N., Tu, N. T., Hung, L. X., ... & Tung, L. A. (2020, November). Multi-objective optimization of surface roughness and MRR in surface grinding of hardened SKD11 using grey-based Taguchi method. *In International Conference on Engineering Research and Applications* (pp. 584-593). *Cham: Springer International Publishing.* https://doi.org/10.1007/978-3-030-64719-3_64

Kadirgama, K. (2021). A comprehensive review on the application of nanofluids in the machining process. *International Journal of Advanced Manufacturing Technology, 115*(9–10), 2669–2681. https://doi.org/10.1007/s00170-021-07316-8

Korkut, I., & Donertas, M. A. (2007). The influence of feed rate and cutting speed on the cutting forces, surface roughness and tool–chip contact length during face milling. *Materials & Design, 28*(1), 308–312. https://doi.org/10.1016/j.matdes.2005.06.002

Kumar, Gaurav, Binayak Sen, Sudarsan Ghosh, and P. V. Rao. (2024). Strategic Enhancement of Machinability in Nickel-Based Superalloy Using Eco-Benign Hybrid Nano-MQL Approach. *Journal of Manufacturing Processes, 127*,457–476. https://doi.org/10.1016/j.jmapro.2024.08.015

Kumar, Mechiri Sandeep, and V. Murali Krishna. (2020). An Investigation on Turning AISI 1018 Steel with Hybrid Biodegradeable Nanofluid/MQL Incorporated with Combinations of CuO-Al2O3 Nanoparticles. *Materials Today: Proceedings, 24*, 1577–84. https://doi.org/10.1016/j.matpr.2020.04.478

Liu, Mingzheng, Changhe Li, Qinglong An, Yanbin Zhang, Min Yang, Xin Cui, Teng Gao, Yusuf Suleiman Dambatta, and Runze Li. (2025). Liquid Film Thickness Model Formed by Atomized Droplets during Sustainable Cryogenic Air MQL Grinding. *Frontiers of Mechanical Engineering, 20*(1), 8. doi:10.1007/s11465-025-0824-8.

Liu, Mingzheng, Changhe Li, Min Yang, Teng Gao, Xiaoming Wang, Xin Cui, Yanbin Zhang, Zafar Said, and Shubham Sharma. (2023). Mechanism and Enhanced Grindability of Cryogenic Air Combined with Biolubricant Grinding Titanium Alloy. *Tribology International 187*, 108704. https://doi.org/10.1016/j.triboint.2023.108704.

Liu, Mingzheng, Changhe Li, Yanbin Zhang, Qinglong An, Min Yang, Teng Gao, Cong Mao, et al. (2021). Cryogenic Minimum Quantity Lubrication Machining: From Mechanism to Application. *Frontiers of Mechanical Engineering, 16*(4), 649–97. doi:10.1007/s11465-021-0654-2.

Lotfi, Bahram, Ramazan Hakkı Namlu, and S. Engin Kılıç. (2024). Machining Performance and Sustainability Analysis of Al2 O3 -CuO Hybrid Nanofluid MQL Application for Milling of Ti-6Al-4V. *Machining Science and Technology, 28(1*), 29–73. doi:10.1080/10910344.2023.2287655.

Mac, T.-B., Luyen, T.-T., & Nguyen, D.-T. (2023). Assessment of the effect of thermal-assisted machining on the machinability of SKD11 alloy steel. *Metals, 13*(4), 699. https://doi.org/10.3390/met13040699

Namlu, Ramazan Hakkı, and Bilgin Kaftanoğlu. (2025). Enhancing Sustainable Machining of Inconel 718 Using Multi-Walled Carbon Nanotubes and TiO2 Based Nanofluid Minimum Quantity Lubrication. *Procedia CIRP, 135*,781–86. https://doi.org/10.1016/j.procir.2024.12.074.

Namlu, Ramazan Hakkı, Bahram Lotfi, and S. Engin Kılıç. (2024). Enhancing Machining Efficiency of Ti-6Al-4V through Multi-Axial Ultrasonic Vibration-Assisted Machining and Hybrid Nanofluid Minimum Quantity Lubrication. *Journal of Manufacturing Processes, 119*,348–71. https://doi.org/10.1016/j.jmapro.2024.03.073

Nguyen, H.-T., & Hsu, Q.-C. (2016). Surface roughness analysis in the hard milling of JIS SKD61 alloy steel. *Applied Sciences, 6*(6), 172. https://doi.org/10.3390/app6060172

Nipu, S. A., Karim, R., Rahman, A., Moon, M., Choudhury, I. A., Omar, J. B., & Khushbu, M. S. (2023). Turning SKD 11 Hardened Steel: An Experimental Study of Surface Roughness and Material Removal Rate Using Taguchi Method. *Advances in Materials Science and Engineering, 2023*(1), 6421918. https://doi.org/10.1155/2023/6421918

Özel, T., & Karpat, Y. (2005). Predictive modeling of surface roughness and tool wear in hard turning using regression and neural networks. *International Journal of Machine Tools and Manufacture, 45*(4–5), 467–479. https://doi.org/10.1016/j.ijmachtools.2004.09.007

Salur, Emin, Nursena Okcu, Mehmet Erdi Korkmaz, Kübra Kaya, Rüstem Binali, and Salih Bilal Çetinkal. (2025). Effect of Cooling/Lubrication Conditions on Machining Performance: An Experimental Investigation of 1040 Steel Under Dry, MQL, and Nano-MQL Environments. *Materials, 18*(17), 4063. https://doi.org/10.3390/ma18174063.

Sreejith, P. S., & Ngoi, B. K. A. (2000). Dry machining: Machining of the future. *Journal of Materials Processing Technology, 101*(1–3), 287–291. https://doi.org/10.1016/S0924-0136(00)00445-3

Stachurski, W., & Nadolny, K. (2018). Influence of the condition of the surface layer of a hob cutter sharpened using the MQL-CCA hybrid method of coolant provision on its operational wear. *International Journal of Advanced Manufacturing Technology, 98*(5–8), 2185–2200. https://doi.org/10.1007/s00170-018-2379-x

Vu, M. H., Hue, P. T. M., Huynh, N. T., & Nguyen, Q. M. (2024). Multi-objective Optimization for Enhanced Material Removal Rate and Reduced Machining Roughness in Hard Turning of SKD61 Alloy Steel. *Mathematical Modelling of Engineering Problems*, *11*(3), 680–688. https://doi.org/10.18280/mmep.110312

Wang, Ziheng, Wei Yang, Zhenjing Duan, Shuaishuai Wang, Yuheng Li, Yuyang Zhou, Jiyu Liu, Jinlong Song, and Xin Liu. (2024). Experimental Study on Cold Plasma Jet (CPJ) Assisted Micro-Milling of 30CrMnSiNi2A. *Intelligent and Sustainable Manufacturing, 1*(2), 10017. https://doi.org/10.70322/ism.2024.10017

Weinert, K., Inasaki, I., Sutherland, J. W., & Wakabayashi, T. (2004). Dry machining and minimum quantity lubrication. *CIRP Annals, 53*(2), 511–537. https://doi.org/10.1016/S0007-8506(07)60027-4

Youssef, H. A., & El-Hofy, H. (2008). Machining technology: Machine tools and operations. CRC Press. https://doi.org/10.1201/9781420043402.

Manuscript Received: 27 September 2025
Revised Manuscript Received: 27 March 2026
Accepted Manuscript: 22 July 2026